DEFENSE TECHNICAL INFORMATION CENTER

Information for the Defense Community

DTIC® has determined on _8 / 10 6 2009_ that this Technical Document has the Distribution Statement checked below. The current distribution for this document can be found in the DTIC® Technical Report Database.

☒ DISTRIBUTION STATEMENT A. Approved for public release; distribution is unlimited.

☐ © COPYRIGHTED; U.S. Government or Federal Rights License. All other rights and uses except those permitted by copyright law are reserved by the copyright owner.

☐ DISTRIBUTION STATEMENT B. Distribution authorized to U.S. Government agencies only (fill in reason) (date of determination). Other requests for this document shall be referred to (insert controlling DoD office)

☐ DISTRIBUTION STATEMENT C. Distribution authorized to U.S. Government Agencies and their contractors (fill in reason) (date of determination). Other requests for this document shall be referred to (insert controlling DoD office)

☐ DISTRIBUTION STATEMENT D. Distribution authorized to the Department of Defense and U.S. DoD contractors only (fill in reason) (date of determination). Other requests shall be referred to (insert controlling DoD office).

☐ DISTRIBUTION STATEMENT E. Distribution authorized to DoD Components only (fill in reason) (date of determination). Other requests shall be referred to (insert controlling DoD office).

☐ DISTRIBUTION STATEMENT F. Further dissemination only as directed by (inserting controlling DoD office) (date of determination) or higher DoD authority.

Distribution Statement F is also used when a document does not contain a distribution statement and no distribution statement can be determined.

☐ DISTRIBUTION STATEMENT X. Distribution authorized to U.S. Government Agencies and private individuals or enterprises eligible to obtain export-controlled technical data in accordance with DoDD 5230.25; (date of determination). DoD Controlling Office is (insert controlling DoD office).

REPORT DOCUMENTATION PAGE

The public reporting burden for this collection of information is estimated to average 1 hour per response, including the time for reviewing instructions, searching existing data sources, gathering and maintaining the data needed, and completing and reviewing the collection of information. Send comments regarding this burden estimate or any other aspect of this collection of information, including suggestions for reducing the burden, to the Department of Defense, Executive Service Directorate (0704-0188). Respondents should be aware that notwithstanding any other provision of law, no person shall be subject to any penalty for failing to comply with a collection of information if it does not display a currently valid OMB control number.

PLEASE DO NOT RETURN YOUR FORM TO THE ABOVE ORGANIZATION.

1. REPORT DATE (DD-MM-YYYY)	2. REPORT TYPE	3. DATES COVERED (From - To)
04-02-2008	Final Report	Jan 2007 - Nov 2007

4. TITLE AND SUBTITLE	5a. CONTRACT NUMBER
A Phased Array Magnetometer for Sensing IED	
	5b. GRANT NUMBER
	FA9550-07-1-0107
	5c. PROGRAM ELEMENT NUMBER

6. AUTHOR(S)	5d. PROJECT NUMBER
Carman, Greg P.; Chang, Chia-Ming	
	5e. TASK NUMBER
	5f. WORK UNIT NUMBER

7. PERFORMING ORGANIZATION NAME(S) AND ADDRESS(ES)	8. PERFORMING ORGANIZATION REPORT NUMBER
The Regents of the University of California Office of Contract and Grant Administration 11000 Kinross Avenue, Suite 102 Los Angeles, CA 90095-1406	

9. SPONSORING/MONITORING AGENCY NAME(S) AND ADDRESS(ES)	10. SPONSOR/MONITOR'S ACRONYM(S)
USAF, AFRL AF Office of Scientific Research 875 N. Randolph St. Room 3112 Arlington, VA 22203	
	11. SPONSOR/MONITOR'S REPORT NUMBER(S)

12. DISTRIBUTION/AVAILABILITY STATEMENT

13. SUPPLEMENTARY NOTES

14. ABSTRACT

A novel magnetometer utilizing a magneto-electric (M-E) laminate was studied. The focus of this research was to analytically and experimentally evaluate the lamination scheme to understand the magneto-electric interactions and comment on its potential for use in detection and identification of improvised explosive devices (IED). A heterogeneous layered magneto-electric system composed of piezoelectric and magnetostrictive constituents were fabricated. UCLA also developed theoretical models necessary to predict magneto-electric behavior and optimize the sensitivity of the resulting material system. Based on this work, the sensitivity of a laminate is expected to exceed 1e-9 Gauss. Analytical modeling suggests this provides defection capabilities of a 0.2 m object up to 80 m away. These highly sensitive magneto-electric laminate elements may eventually be integrated into array architectures to provide three dimensional detection at relatively large standoff distances.

15. SUBJECT TERMS

magneto-electric materials, piezoelectric, magnetostrictive, magnetometer, improvised explosive device (IED), shear lag, demagnetization

16. SECURITY CLASSIFICATION OF:			17. LIMITATION OF ABSTRACT	18. NUMBER OF PAGES	19a. NAME OF RESPONSIBLE PERSON
a. REPORT	b. ABSTRACT	c. THIS PAGE			
					19b. TELEPHONE NUMBER (Include area code)

Standard Form 298 (Rev. 8/98)
Prescribed by ANSI Std. Z39.18
Adobe Professional 7.0

Air Force Office of Scientific Research (AFOSR)

Annual Final Report

Mechanical and Aerospace Engineering Department
University of California, Los Angeles
Los Angeles, CA 90095-1597
Voice: 310-825-6030
Fax: 310-206-2302

Funding Organization	**USAF/Office of Scientific Research & Joint Improvised Explosive Device Organization (JIEDDO)** (Contract No: **FA9550-07-1-0107**)
Program Manager	**Dr. Byung-Lip "Les" Lee**
Project Title	**A Phased Array Magnetometer for Sensing IED**
Total Funding	133,000.00
Project Period	01/2007 ~ 12/2007
Key Personnel	Principal Investigator: Greg P. Carman, Ph.D.
	Research Associate: Chia-Ming Chang, Graduate Student
	Tien-Kan Chuang, Graduate Student

1

A Sensitive Phased Array Magnetometer for Sensing IED

Greg P. Carman, Chia-Ming Chang, and Tien-Kan Chung
Mechanical and Aerospace Engineering Department
University of California Los Angeles
Los Angeles, CA 90095-1597
Voice: 310-825-6030
Fax: 310-206-2302

1. OVERALL OBJECTIVE

The objective of this project was to develop the fundamental knowledge to enable a novel technology for detecting and identifying improvised explosive devices (IED). A magnetometer array having the advantages of high sensitivity, compact size and low power consumption were utilized to advance sensing technology and enable sensitive measurements. A heterogeneous layered magneto-electric system composed of piezoelectric and magnetostrictive constituents were made to develop a platform that could sense magnetic fluctuations in earth magnetic fields.

The most challenging but promising characteristics of magneto-electric laminate composites is large sensitivity in a relatively small package including electronics. In order to optimize the M-E based magnetometer, precise theoretical modeling, sophisticated experimental confirmation, along with fabrication technology was required.

During this program, UCLA developed theoretical models necessary to predict magneto-electric behavior for the layered composites and optimize the structure. Based on this analytical framework, the sensitivity of a laminate is expected to exceed 1×10^{-9} Gauss This potentially provides defection capability of a 0.2 m object up to 250 feet away. These highly sensitive magneto-electric laminate elements may eventually be integrated into array architectures to provide three dimensional detection of spatial magnetic field distribution. With this innovative technology, the distance and direction of the IED and other dangerous munitions can possibly be detected at safe standoff distances.

2. STATUS OF EFFORT

In this section, the system's working philosophy for magneto-electric magnetometer is described. The efforts including theoretical analysis, sample fabrication, and test confirmation, specifically the class of magneto-electric materials, are subsequently discussed. The magneto-electric materials are layered piezoelectric with magnetostrictive materials. To successfully accomplish the objective, UCLA developed analytical models to predict the response of heterogeneous layered magneto-electrics. In addition, UCLA fabricated and tested heterogeneous layered materials to validate the analytical models.

2.1 System Description

In this study, the sensing mechanism for a phased array magneto-electric magnetometer is based on the magneto-electric (M-E) coupling, which is defined as the dielectric polarization P when subjected to a magnetic field H. The fundamental

phenomenon associated with this material is completely different from traditional coil-based sensing approaches. The M-E coupling appears in the constitutive equations and is thus present even at quasi-static excitations. Eq. [1] shows the basic constitutive relations contracting the M-E materials relations with "conventional" materials. The ε and μ are the permittivity and the permeability of the dielectric materials the ferromagnetic materials, respectively. However, there is an additional term α in the magneto-electric equations which represents the coupling suggested by Debye, i.e. a magnetic field produces an electric flux (D) in the first of Eq. [1] left or conversely a electric field produce a magnetic flux (B) in the second of Eq. [1] left. This clearly indicates that the presence of a magnetic field (H) produces an electric charge (D) through the coupling term α. **That is, the magneto-electric materials can be used to detect the presence of small changes in magnetic fields**.

<div align="center">

MAGNETO-ELECTRIC   **CONVENTIONAL**

$D = \varepsilon E + \alpha H$ $D = \varepsilon E$

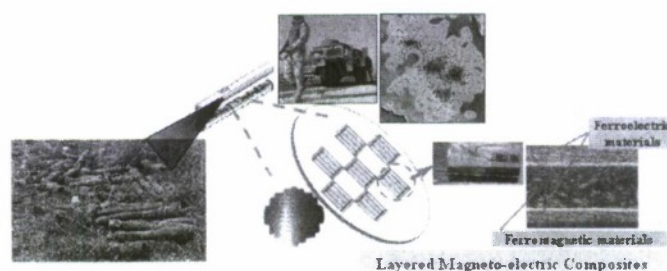$B = \mu H + \alpha E$ $B = \mu H$ [1]

</div>

Figure 1. Magneto-electric based magnetometer for detecting IED

Among all types of M-E materials, the layered configuration has been proved to exhibit the maximum M-E coupling. The focus of this report is on understanding the

response of individual elements (see Fig. 1 circled region) used in a phased array approach to image IED. A layered M-E element contains layered piezoelectric/magnetostrictive materials to transfer information between magnetic and electrical energies using mechanical transduction. The incoming electromagnetic waves drive the magnetostrictive materials and produce dynamic strains in the magnetostrictive material inducing a voltage in the piezoelectric. The time varying voltage provides information concerning the surrounding electro-magnetic environment, i.e. disturbances produced by IED. Piezoelectric and magnetostrictive materials are chosen for the multiferroic material due to their extreme sensitivities to small disturbance.

2.2 Methodology and Status of Effort

Three major tasks, quasi-static modeling, fabricating, and testing the combined electro-magnetic-mechanical response of an individual element have been accomplished for use as a magnetometer. In the following three sections a brief review of achievements on each of these related topics is described. The first section describes the analytical modeling efforts on quasi-static model. The second section introduces the fabrication and test setup for magneto-electric materials. Excellent agreement is found between analytical and experimental results. Following this, the third and final section describes the potential sensitivity and range for a magnetometer fabricated with the magneto-electric laminate. This section addresses the sensitivity to detect IED with the conclusion that considerable standoff distances 1000 feet may be achieved.

2.2.1 Modeling Element Response

An analytical framework has been developed for optimizing the performance of magneto-electric based magnetometers. A quasi-static model is developed to determine the best combinations of ferroelectric (i.e. piezoelectric) and ferromagnetic (i.e. magnetostrictive) layers, sample geometry, and field orientations to maximize the M-E coupling. In addition, the model includes a shear lag analysis to account for mechanical coupling present near free edges and demagnetizing effects present in ferromagnetic materials due to the continuity conditions at the boundary.

2.2.1.1 Quasi-static Uniform Strain Model

UCLA focused on optimizing the sensitivity of layered magnetoelectrics to detect spatial magnetic fields. A quasi-static theoretical model was developed for predicting the magneto-electric (M-E) voltage coefficient α for a ferromagnetic-ferroelectric (i.e. magnetostrictive-piezoelectric layered M-E material). The fundamental equations for the layered system are provided below.

$$
\begin{aligned}
&\text{Poled piezoelectric Phase:} &&\text{Magnetostrictive Phase:} \\
&{}^{P}\varepsilon_{ij} = {}^{P}s_{ijkl}\,{}^{P}\sigma_{kl} + {}^{P}d_{kij}\,{}^{P}E_{k} &&{}^{m}\varepsilon_{ij} = {}^{m}s_{ijkl}\,{}^{m}\sigma_{kl} + {}^{m}q_{kij}\,{}^{m}H_{k} &&[2]\\
&{}^{P}D_{i} = {}^{P}d_{ikl}\,{}^{P}\sigma_{kl} + {}^{P}\in_{ij}\,{}^{P}E_{j} &&{}^{m}B_{i} = {}^{m}q_{ikl}\,{}^{m}\sigma_{kl} + {}^{m}\mu_{ij}\,{}^{m}H_{j}
\end{aligned}
$$

Where d_{kij} and $\in_{ij}$ are piezoelectric coefficients and permittivity; q_{kij} and μ_{ij} are piezomagnetic coefficients and permeability; and S_{ijkl} is the compliance matrix. This coupling arises when the two materials are mechanically bonded to form magneto-electric energy exchange. In addition, Eq. [3] shows the full coupling of the homogenized magneto-electric system.

$$\varepsilon_{ij} = s_{ijkl}\sigma_{kl} + d_{kij}E_k + q_{kij}H_k$$
$$D_i = d_{ikl}\sigma_{kl} + \in_{ij} E_j + \alpha_{ij}H_j \qquad [3]$$
$$B_i = q_{ijk}\sigma_{jk} + \mu_{ij}H_j + \alpha_{ij}E_j$$

Considering combinations of sample geometry, material property, and field orientation of the individual layers, one can summarize the six fundamental system configurations for a magnetometer as shown in Fig. 2.
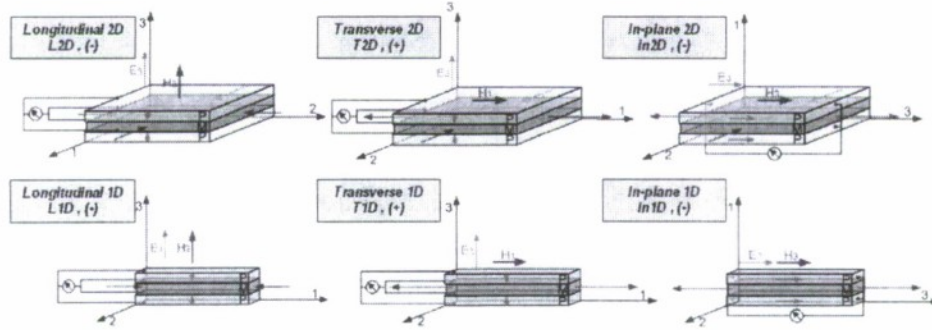

Figure 2. Six fundamental M-E laminate composites configurations

The theoretical modeling of each fundamental case provides the necessary information to optimize the static response of a magnetometer.

By using the constitutive equations for layered system Eq. [2] along with homogenized material Eq. [3] and considering plate theory and essential conditions for various fundamental configurations, the M-E voltage coefficients are solved to quantify the M-E coupling for each lay up. Eq. [4] shows the α solution for one particular lay up in which the orientations of incident magnetic field and measuring electric field are both in plane.

$$\alpha_{33}^{In2D} = \frac{E_3}{H_3} = \frac{\begin{array}{l}{}^m v({}^P s_{33}{}^P d_{32}{}^m q_{32}{}^m v + {}^P s_{22}{}^P d_{33}{}^m q_{33}{}^m v - {}^P s_{23}({}^P d_{33}{}^m q_{32} + {}^P d_{32}{}^m q_{33}){}^m v + \\ ({}^m s_{33}{}^P d_{32}{}^m q_{32} - {}^m s_{23}{}^P d_{33}{}^m q_{32} - {}^m s_{23}{}^P d_{32}{}^m q_{33} + {}^m s_{33}{}^P d_{33}{}^m q_{33}){}^P v)\end{array}}{\begin{array}{l}{}^m v({}^P s_{33}{}^P d_{32}{}^{2}{}^m v - 2{}^P s_{23}{}^P d_{32}{}^P d_{33}{}^m v + {}^m s_{33}{}^P d_{32}{}^{2}{}^P v + \\ {}^P d_{33}({}^P s_{22}{}^P d_{33}{}^m v - 2{}^m s_{23}{}^P d_{32}{}^P v + {}^m s_{33}{}^P d_{33}{}^P v)) + (({}^P s_{23}{}^{2} - {}^P s_{22}{}^P s_{33}){}^m v^2 - \\ (-2{}^m s_{23}{}^P s_{23} + {}^m s_{33}({}^P s_{22} + {}^P s_{33})){}^m v^P v + ({}^m s_{23} - {}^m s_{33})({}^m s_{23} + {}^m s_{33}){}^P v^2) \in\end{array}} \qquad [4]$$

As one can see from the arguments in this particular α equation, they are geometrically and material dependent. By choosing a specific material, one can increase the magnetometer's sensitivity to detect changes in magnetic fields provided by variety of objects including IED's.
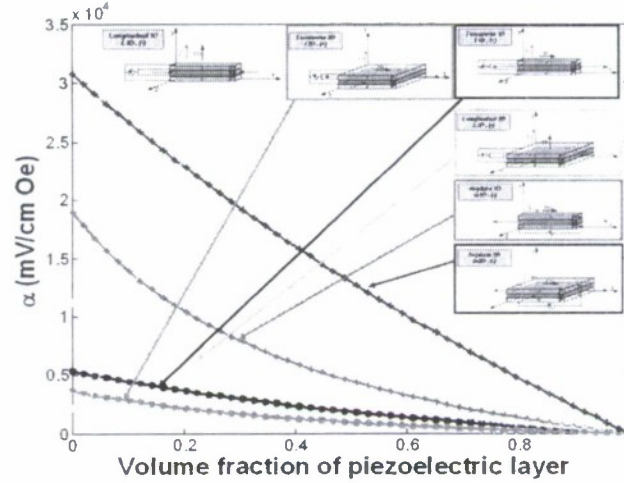

Figure 3. Terfenol-D + PZT-5H α as a function of volume fraction

Fig. 3 plots the M-E voltage coefficient α as a function of PZT-5H volume fraction for each configuration. The curves indicate that α for each configuration reaches the maximum when the minimum piezoelectric amount is used in the system. **This suggests one should minimize the volume fraction of piezoelectric materials to reach the highest sensitivity for magnetometer**. Also, notice that each configuration has different α performance that may be further influenced by material properties such as Young's modulus (Y), piezoelectric (d) and piezomagnetic (q) coefficients and field orientations

8

(see Eq. [4]). For the case shown in Fig. 3, the **in plane-2D case**, with both PZT polarization and magnetic field being in plane direction of a two dimensional sample, **is the best choice for a sensitive magnetometer**. Furthermore, when reviewing the results, the coefficient α for this particular material system can vary from a low of less than 2000 mV/(cm Oe) up to a value of 300,000 mV/(cm Oe). The result demonstrates that an order of magnitude increases from what has previously reported is possible if the system is constructed using analytical guidance. That is previous researchers used intuition to fabricate samples rather than analytical models. Therefore, the geometry, configuration, and material selection are of primary importance to maximize the coupling coefficients or sensitivity.

While the results shown in Fig. 3 represent one particular material system, we conducted an optimization which will be used to determine the appropriate materials for the heterogeneous layered system for practical fabrication. During this study we investigated the influence of different materials (i.e. different piezomagnetic coefficient q_{33} and the ratio q_{33}/q_{31} (see Eq. [2])). UCLA was able to demonstrate that the ratio q_{33}/q_{31} was a component that strongly influences the selection of layered heterogeneous configuration to maximize the sensitivity of the α. From these results UCLA concluded that the most likely candidate material for the magnetometer is a hard ferroelectric material to minimize losses but with a **large piezoelectric coefficient** such as a lead titanate, lead zirconate, or lithium niobate and magnetostrictive materials such as Nickel Iron (i.e. Mu-metal and Permalloy), Metglas, or Cobalt Nickel CoNi with **high piezomagnetic coefficients** instead of large magnetostriction. Using a particular subset

of these materials in the model, the α value can be increased by an order of magnitude (i.e. 200,000 mV/(cm Oe)). Based on the model at the end of this proposal, this value provides sufficient sensitivity to enable the detection of $1 \times 10^{-11} \sim 1 \times 10^{-6}$ Gauss magnetic flux density (B) for a magneto-electric laminate system.

2.2.1.2 Quasi-static Shear Lag & Demagnetization Model

In the previous section, the uniform strain theory provided qualitative guidance to predict both the M-E voltage coefficient and the strain values as a function of material properties and dimensional factors. This section further considers the M-E samples with finite length in which non-uniform strains are developed particularly near the free edges due to mechanical shear lag effect and demagnetization. Accordingly, the shear lag plus demagnetization model is required to quantitatively predict the M-E coupling for the layered M-E elements by considering the end effects for the finite M-E samples.

For mechanical shear lag, material properties, sample geometry for piezoelectric/magnetostrictive plates and also bonding layers were considered. By solving displacement-strain relationship, force equilibrium, and constitutive equations for all layers, the strain distribution equations along the sample length was obtained. For the demagnetizing effect of the magnetostrictive plate, the effect magnetic field inside the material is derived as a function of material properties and sample geometries. By combining shear lag and demagnetization equations with essential boundary strain conditions, the shear lag and demagnetization modeling is developed as shown in Eq. [5].

$$\begin{bmatrix} {}^{p}\varepsilon_{11} \\ {}^{m}\varepsilon_{11} \end{bmatrix} = \begin{bmatrix} 1 \\ 1 \end{bmatrix} \frac{\Psi\Omega_{eff}}{\Psi + 2K} + \begin{bmatrix} \dfrac{-\Psi}{2K} \\ 1 \end{bmatrix} \frac{2K\Omega_{eff}}{(\Psi + 2K)\cosh\Gamma} \cosh\overline{\Gamma x} \qquad [5]$$

Where the prime quantities represent differentiation with respect to a non-dimensional coordinate $\bar{x} \equiv x/(L/2)$. The Γ is the shear lag parameter containing non-dimensional parameters of $\bar{G} \equiv G/{}^{p}Y_{11}$, piezoelectric modulus K, $\theta_b \equiv {}^{b}t/{}^{p}t$, $\overline{{}^{p}t} \equiv {}^{p}t/(L/2)$, and stiffness ratio $\Psi \equiv {}^{m}Y_{11}{}^{m}t/{}^{p}Y_{11}{}^{p}t$. The effective magneto-electric voltage coefficient $\bar{\alpha}$ can be obtained by averaging the values of the point-wise distributed α.

$$\bar{\alpha} = \frac{1}{\overline{V}} \iiint_V \alpha(\bar{x}) d\bar{x} d\bar{y} d\bar{z} \qquad [6]$$

The three prime non-dimensional parameters including shear lag parameters (Γ), stiffness ratios (Ψ), and demagnetizing parameters (Λ_d) are used to parametrically study the influences caused by material properties and sample geometries on the M-E performances. The results indicate that shear lag and demagnetizing effects cause substantial strain decay near the free ends while demagnetizing effects decrease the far-field strain values also. By using a longer sample with a thinner and stiffer bonding layer (implying larger Γ), the shear lag effects are minimized. When a magnetostrictive layer with smaller relative permeability μ_r values and higher aspect ratios (implying larger Λ_d) are used, the demagnetization becomes less significant. Moreover, a relatively thicker and stiffer magnetostrictive layer (implying larger Ψ) increases the far-field strain values. In general, larger Γ, Ψ, and Λ_d values produce more uniform and higher strains that increase the effective $\bar{\alpha}$ values. A detailed comparison with experiments is introduced in a subsequent section entitled "*Theory and Test Agreement*."

11

2.2.2 Fabrication and Testing Various Individual Element

2.2.2.1 Sample fabrication

Fig. 4 illustrates the fabrication process for a 1-3 type Terfenol-D material used in a prototype magneto-electric laminate. The Terfenol-D composite is illustrated in Fig. 4(a). This step involves the mixture of 55% by volume Terfenol-D particulates with a size of 50~300 μm (ETREMA Products, Inc., Ames, IA) with a Vinyl ester resin (Dow Derakane 411-C50) in a Plexiglas mold with a cavity of $24.45 \times 14.45 \times 12.55$ mm^3. After firmly taping the cover, the mold is placed between a pair of electromagnets producing a uniform magnetic field of 150 kA/m to align the particulates while curing the Vinyl ester resin at 70 °C. Fig. 4(a) shows the Terfenol-D composite after demolding and Fig. 4(b) shows the subsequent sample preparation for the magnetostrictive material characterization. The characterization shown in Fig. 4(b) provides necessary material properties including elastic moduli ($^mY_{11}$, $^mY_{22}$), piezomagnetic coefficients ($^mq_{11}$, $^mq_{12}$), and relative permeability (μ_r) for input into the M-E model.
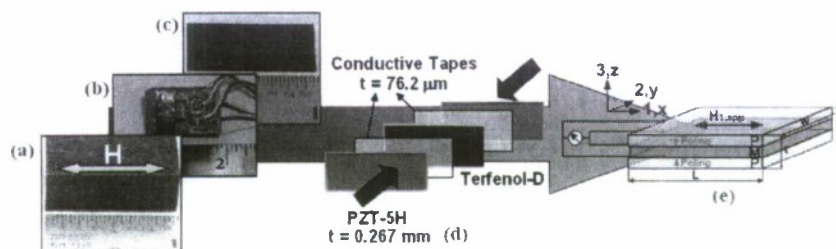

Figure 4. Schematic of Terfenol-D composite characterization and subsequent fabrication of layered magneto-electric samples

Fig. 4(c) illustrates the magnetostrictive slice used to fabricate the magneto-electric based magnetometer element. As shown in Fig. 4(d), each M-E laminate element was

fabricated by sandwiching a magnetostrictive layer between two oppositely poled ferroelectric plates to enable the magneto-electric operation. The piezoelectric layers were electrically connected in parallel, Fig. 4(e), to monitor the voltage/charge produced.

2.2.2.2 Test Setup

The previous two sections described the modeling and fabrication of individual elements. The following task focuses on experimentally evaluating the response of the heterogeneous layered M-E element.
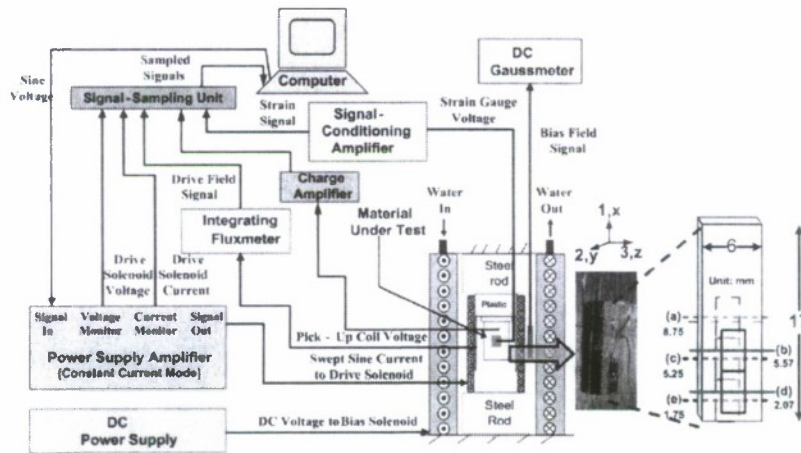

Figure 5. Schematic test setup of magneto-electric voltage coefficient measurement for a heterogeneous layered multiferroic

A schematic of the critical components and approach to evaluate an M-E sample are provided in Fig. 5. The tests conducted on the heterogeneous system provide critical information on the sensitivity as well as the response of the system. Quasi-static tests provided M-E voltage coefficients. The M-E sample was placed inside two solenoids: An inner (driving) solenoid for generating an AC magnetic field and an outer (bias) solenoid for providing a DC magnetic field bias. A computer-based controller was used

to drive solenoid and record the signal from the testing system. The magnetic fields, including H_{bias} and $H_{1,ac}$, were applied in 1 direction without mechanical loading. H_{bias} was measured with a Hall-effect gaussmeter (F.W. Bell 5080) placed adjacent to the middle of the sample. Magnetic flux density (B_1) was measured by a pick up coil situated around the M-E sample with a fluxmeter. The voltage induced across the PZT-5H layer was measured using a high resistance charge amplifier (Kistler Instrument 5010B) which essentially produces an open-circuit condition.

2.2.2.3 Theory and Test Agreement

Only a small subset of data is presented in this section. For the case of $H_{bias} = 750$ Oe, Fig. 6 plots the measured strain distribution (Points A ~ E) as a function of normalized position ($\bar{x}$). In the figure, experimental data along with the theoretical prediction using uniform strain theory, shear lag only (Eq. [5] without demagnetization), and shear lag plus demagnetization model (Eq. [5]) are compared. The measured strains exhibit a tent-shaped distribution which is close to zero near the edges (i.e. $\bar{x} = \pm 1$) and climbs to a far-field value of 24.4 με near the sample middle point (i.e. $\bar{x} = 0$), while the homogeneous solution predicts a uniform strain of 29.0 με though the sample. As shown in Fig. 6, an analysis which only includes shear lag predicts a decaying strain with position. Although the shear lag model presents a similar strain profile with the test data and approaches the theoretical uniform strain at the middle of the sample, the strain distribution shows substantial differences with the test data. When demagnetization is incorporated into the shear lag model (Eq. [5]), general agreement with test data is observed throughout the sample. Particularly, the far-field strain of 25.7 με is only 5%

larger than test data. The excellent correlation implies that neither shear lag nor demagnetization effects can be ignored for predicting M-E coupling. Because the spatially varying strain produces a position dependent electric field, the effective M-E voltage coefficient, $\bar{\alpha} = \delta\bar{E}/\delta H$, for the M-E laminate composites is also impacted.
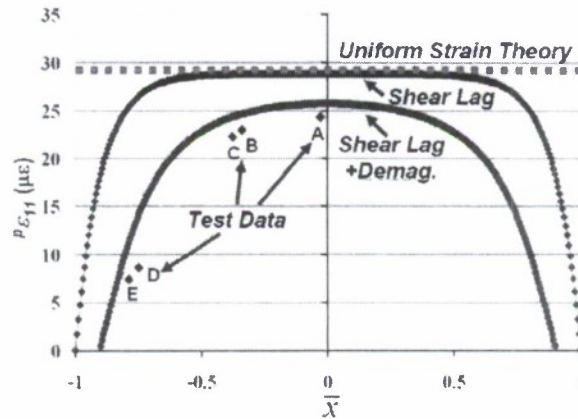

Figure 6 Piezoelectric strain distribution for theoretical predictions and experimental data at

Hbias = 750 Oe of ^Pv = 0.17

Fig. 7 shows a comparison of theoretical predictions and experimental measurements. The purpose of this comparison is to ensure the appropriate assumptions are used in developing the analytical models so that future researchers are provided with fundamental tools. Comprehensive comparisons have been made between experimental measurements and theoretical results for strain distribution and effective M-E voltage coefficient α. A number of three piezoelectric volume fractions, ^Pv = 0.17, 0.28, and 0.44 for M-E laminate composites were studied. The small variation between experimental measurements and theoretical predictions, i.e. less than 5%, clearly demonstrates that the analysis accurately predicts the developed M-E voltage coefficient α in the M-E sample.
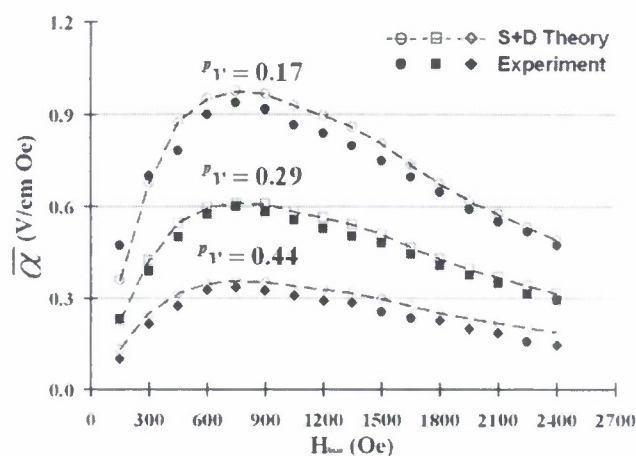
15

Figure 7 The agreement of quasi-static modeling and experimental results for transverse case

2.2.3. CAPABILITY ADDRESSED

The purpose of this research was to develop the fundamental basis to enable a new approach for detecting Improvised Explosive Devices (IED) on the battlefield. Based on the data described and an analytical model, the M-E laminate may be able to detect a 0.2 m radius IED at a distance of 80 m (240 feet).

In order to understand the distribution of a magnetic flux density (B) as a function of distance from an IED, we simplify the magnetic induction system for IED by assuming the disturbance produced by the IED can be represented by current loop (i.e. a ring). Fig. 8 shows a schematic concept and the Biot-Savart Law relating the magnitude of *dB* contributed by any length element *ds*.

$$dB = \frac{\mu_0 I}{4\pi} \frac{\left| ds \times \hat{r} \right|}{r^2} = \frac{\mu_0 I}{4\pi} \frac{ds}{(x^2 + R^2)}$$
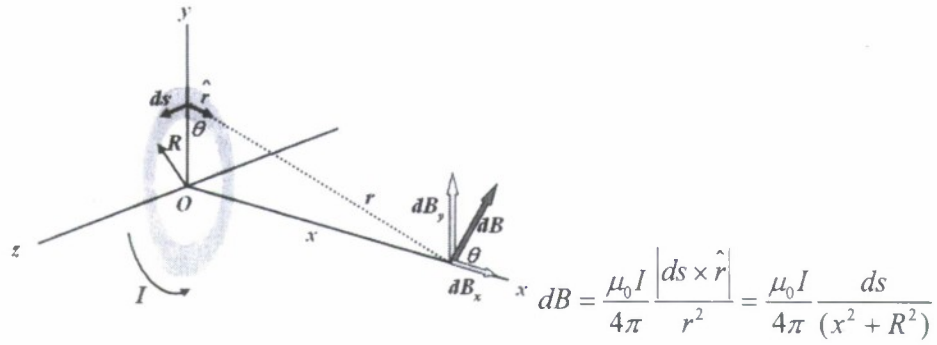
Figure 8. Schematic for calculating the magnetic flux density (B) along the axis.

Because the resultant dB_x for all elements around the loop is equal to zero, the equation above can be reduced to:

$$B_x = \frac{\mu_0 I}{4\pi} \frac{R}{(x^2 + R^2)^{3/2}} \oint ds = \frac{\mu_0 I}{2} \frac{R^2}{(x^2 + R^2)^{3/2}}$$

If $x \square R$, we can further reduce the equation to

$$B_x = \frac{\mu_0 I R^2}{2x^3} \ \text{(For } x \square R \text{)}$$

According to this equation, the magnetic flux density along the axis direction is proportional to the square of current loop radius and decreases rapidly with the cubic of distance x from the end of the IED. By taking steel ($\mu_r = 700$) as an example, we plot the flux density for an IED with different radii ranging from 0.1 ~0.5 m as a function of detecting distance.
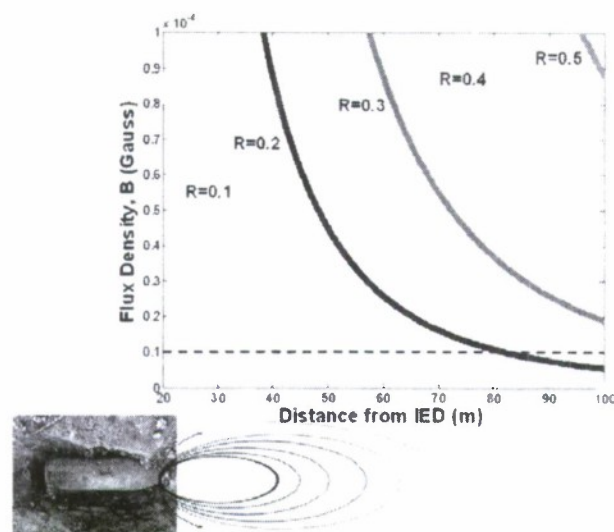
17

Figure 9. The magnetic flux density distribution as a function of distance away from the IED for various IED with different radii

As shown in the figure, the flux density (B) decays with the distance x while it decreases more slowly for IED with larger dimension. This indicates that the perturbations is the signal from larger IED and can be detected at greater distance. If the detectable level is 1×10^{-5} Gauss as illustrated in dashed line, a 0.2 m radius IED can be detected up to 80 meters (240 feet) far! This dramatically increase the detectable distance and hence protect the warriors and equipment in the battle field.

3. ACCOMPLISHMENTS:

1. Analytically studied magneto-electric laminate system to optimize structural sensitivity of the magneto-electric laminate composites.

2. Developed the first accurate model including shear lag and demagnetization effects which incorporates the end effects for layered magneto-electric elements with finite length.

3. Fabricated magneto-electric laminates based on analytical models.

4. Experimentally tested and confirmed the magneto-electric coupling including end effects for the "bulk" magneto-electric system.

5. Developed a rudimentary predictive approach to suggest what size an IED can be defected at different stand-off distances.

4. PERSONNEL SUPPORTED

Principle investigator: Professor Gregory P. Carman

Graduate Student Researcher: Chia-Ming Chang, Tien Kan Chung

5. PUBLICATIONS

Journals:

1. Chia-Ming Chang and Gregory P. Carman, "Experimental evidence of end effects in magneto-electric laminate composites", *Journal of Applied Physics*, 2007, 102, 124901, 2007.

2. Chia-Ming Chang and Gregory P. Carman, "Modeling shear lag and demagnetization effects in magneto-electric laminate composites", *Physical Review B*, 76, 134116, 2007.

3. Chia-Ming Chang and Gregory P. Carman, "Analytically evaluating the properties and performance of layered magneto-electric composites", *Journal of Intelligent Material Systems and Structures*, 085410, 2007.

Conference proceedings:

1. Chia-Ming Chang and Gregory P. Carman, "End Effects of Finite Magneto-Electric Laminate Composites", Proc. SPIE, 2008, In Press.

2. Tien Kan Chung, Kotekar P. Mohanchandra, Chia-Ming Chang and Gregory P. Carman, "A novel Evaluation of Piezoelectric Coefficient of PZT think Film", Proc. SPIE, 2008, In Press.

6. INTERACTIONS/TRANSITIONS

Conference/University Presentation:

1. "End Effects of Finite Magneto-Electric Laminate Composites", 2008 SPIE International Symposium: Smart Structure and Materials, San Diego, California, USA (2008).

2. "A novel Evaluation of Piezoelectric Coefficient of PZT think Film", 2008 SPIE International Symposium: Smart Structure and Materials, San Diego, California, USA (2008).

3. "Coupling Effect of Finite Magneto-Electric Laminate Composites", 2007 Structural & Solid Mechanics Research Seminar Series, University of California at Los Angeles,

California, USA (2007).

4. "Prediction of Magneto-electric Coupling Effect in Magneto-Electric Laminate Composites", 2007 SPIE International Symposium: Smart Structure and Materials, San Diego, California, USA (2007).

5. "Magneto-Mechanical Testing of Terfenol-D Bulk and 1-3 Composites", 2007 SPIE International Symposium: Smart Structure and Materials, San Diego, California, USA (2007).

7. HONORS/AWARDS

→ BEST PAPER AWARD

Material category, American Society of Mechanical Engineers (ASME): Selected best paper published in either a journal or conference proceedings during the year 2007.